

Oxygen versus nitrogen co-ordination in complexes of Mo^{VI} and hydroxamate derivatives of α -amino acids: equilibrium, structural and theoretical studies†

Etelka Farkas,^{a*} Hajnalka Csóka,^a Gareth Bell,^b David A. Brown,^b Laurence P. Cuffe,^b Noel J. Fitzpatrick,^b William K. Glass,^b William Errington^c and Terence J. Kemp^c

^a Department of Inorganic and Analytical Chemistry, Lajos Kossuth University, Debrecen, Hungary. E-mail: farkase@tigris.klte.hu

^b Department of Chemistry, University College, Belfield, Dublin 4, Ireland

^c Department of Chemistry, University of Warwick, Coventry, UK CV4 7AL

Received 30th March 1999, Accepted 22nd June 1999

Equilibrium and spectroscopic studies showed that Mo^{VI} (MoO₄²⁻) reacts with α -aminohydroxamic acids (glycine-, sarcosine-, α -alanine-hydroxamic acids, Glyha, Sarha and α -Alaha) in the acidic pH range to give species involving O,O co-ordination whereas, as the pH is raised, species involving N,N co-ordination are formed. The crystal structure of [MoO₂(Glyha)₂] confirmed formation of an O,O co-ordination isomer. Theoretical studies of the O,O and N,N isomers of [MoO₂(Glyha)₂] and [MoO₂(Sarha)₂] showed the former to be the more stable but the relative closeness of the calculated energies of the isomers is in accord with the solution studies. Histidine hydroxamic acid (Hisha) forms O,O isomers in the acidic pH range but as the pH is raised forms two new isomers, one containing the amino nitrogen protonated and co-ordinated in a tridentate manner using the two hydroxamate oxygen atoms and the imidazole N while the other probably contains protonated imidazole N and is co-ordinated *via* the amino and hydroxamate nitrogens.

Introduction

Molybdenum plays an important role in biological systems especially in the nitrogen fixation process. It has been suggested that siderophores may be involved not only in the uptake of iron by nitrogen-fixing bacteria but also in the transport of molybdenum.¹ This suggestion has accentuated studies of molybdenum(vi)-catecholate and -hydroxamate systems.¹⁻⁶ Our recent equilibrium studies of complexation between molybdenum(vi) and some hydroxamate based ligands^{5,6} led to the following main conclusions: the formation of hydroxamate type chelates (O,O bonding to metals) competes with hydrolytic processes of molybdenum(vi) in the acidic pH range whereas in the neutral and basic pH range the metal ion exists only as [MoO₄]²⁻. Formation of the complex species [MoO₂A₂] (where HA denotes a hydroxamic acid, e.g. acetohydroxamic acid, Aha) occurs at quite acidic pH values (below *ca.* pH 3) and other species, mono(hydroxamato)trioxomolybdenum(vi), [MoO₃A]⁻, exist in the pH range *ca.* 3–6.⁶ The presence of normal chelation through O,O co-ordination in the complex [MoO₂A₂] was confirmed by crystal structure determination for the cases HA = CH₃(CH₂)_nCONHOH (*n* = 4 or 5).⁴ Interestingly, the same species containing the MoO₂²⁺ core plus two hydroxamate chelates is exclusively formed in the molybdenum(vi)-desferrioxamine B system below pH *ca.* 5.5.⁵ (This ligand is a trihydroxamate type siderophore containing the third hydroxamic acid moiety in the above complex in nonco-ordinated and protonated form.)

In the case of hydroxamate ligands containing an amino group situated in β position to the hydroxamate moiety (e.g. β -alanine hydroxamic acid, β -Alaha) co-ordination still occurs

in the “monohydroxamate type”, O,O co-ordination mode with the ligand containing the amino group in its protonated form.⁶

To the best of our knowledge, no studies of molybdenum(vi) complexes of α -aminohydroxamic acids have been reported; however, a number of such complexes with transition metals such as nickel(II), copper(II) and cobalt(II) have been characterised and the presence of N,N co-ordination involving the hydroxamate N and the α -amino N confirmed by crystal structure determinations.^{7,8} Although, co-ordination of the amino N was not found in complexes formed with typically hard metal ions (iron(III), aluminium(III) or gallium(III)) its electronic effect caused a considerable decrease in the stability of the (O,O) hydroxamate chelate.⁹

Complexation between molybdenum(vi) and α -aminohydroxamates has been studied in the present work with glycine hydroxamic acid (Glyha) selected as the simplest representative of the α -aminohydroxamic acids. The effects of the methyl substituent on the α -carbon and on the amino nitrogen have been studied in the molybdenum(vi)- α -alanine hydroxamate (α -Alaha) and -sarcosine hydroxamate (Sarha) systems.

The imidazole nitrogens of histidine-containing bioligands often play a role as co-ordinating donors in various biological systems leading to a widespread interest in metal complexation of different histidine derivatives.¹⁰ Accordingly, histidine hydroxamic acid (Hisha) has also been studied in the present work.

Experimental

The molybdenum(vi) stock solution was prepared from Na₂MoO₄ (Reanal product). The metal ion concentration was checked gravimetrically *via* precipitation of the quinolin-8-olate.

The aminohydroxamic acids were prepared by mixing ice-cold aqueous solutions of the amino acid ester hydrochloride (0.01 mol) and hydroxylamine hydrochloride (0.01 mol), slow

† Supplementary data available: elemental analyses. For direct electronic access see <http://www.rsc.org/suppdata/dt/1999/2789/>, otherwise available from BLDSC (No. SUP 57594, 1 pp.) or the RSC Library. See Instructions for Authors, 1999, Issue 1 (<http://www.rsc.org/dalton>).

Table 1 Stoichiometry and logarithmic stability constants for the proton and molybdenum(vi) complexes formed in the studied systems (25 °C; $I = 0.2 \text{ mol dm}^{-3}$ (KCl))

Equilibrium process	Species	log β					
		α -Alaha	Glyha	Sarha	Hisha	β -Alaha ^a	Aha ^a
$A^- + H^+$	AH	9.19(1)	9.17(1)	9.30(1)	9.06(2)	9.59(1)	9.28(2)
$A^- + 2H^+$	AH ₂ ⁺	16.60(2)	16.64(1)	16.86(1)	16.15(3)	17.91(1)	—
$A^- + 3H^+$	AH ₃ ²⁺	—	—	—	21.61(4)	—	—
$MoO_4^{2-} + 2A^- + 8H^+$	$[MoO_2(AH_2)_2]^{4+}$	—	—	—	55.1(2)	—	—
$MoO_4^{2-} + 2A^- + 7H^+$	$[MoO_2(AH)(AH_2)]^{3+}$	—	—	—	52.88(8)	—	—
$MoO_4^{2-} + 2A^- + 6H^+$	$[MoO_2(AH)_2]^{2+}$	45.90(2)	47.06(6)	47.04(5)	48.5(2)	49.76(5)	—
$MoO_4^{2-} + A^- + 3H^+$	$[MoO_3(AH)]$	24.00(2)	24.43(3)	24.52(2)	24.77(8)	25.81(4)	—
$MoO_4^{2-} + A^- + 2H^+$	$[MoO_3A]$	18.65(4)	19.15(3)	19.48(2)	18.44(8)	—	17.16(4)
$MoO_4^{2-} + 2A^- + 4H^+$	$[MoO_2A_2]$	—	—	—	—	—	32.46(2)

^a Data taken from ref. 6.

addition of 12 mol dm^{-3} sodium hydroxide (0.33 mol), and subsequent acidification with 12 mol dm^{-3} hydrochloric acid.¹¹ When the mixture was cooled the aminohydroxamic acids crystallised easily, and washing with a little cold water gave pure crystals of the aminohydroxamic acid: yield 40%. Satisfactory microanalyses were obtained for the compounds (SUP 57594). All commercial chemicals used in this work were of reagent grade.

The pH-metric and spectrophotometric measurements were carried out at an ionic strength of 0.2 mol dm^{-3} (KCl). Carbonate-free KOH solutions of known concentrations (*ca.* 0.2 mol dm^{-3}) were used as titrant. The HCl stock solutions were prepared from concentrated HCl (Merck) and their concentrations determined by pH-metric titrations. A Radiometer pHM64 instrument equipped with a CTWL 45244/2 combined electrode and an ABU13 burette was used. The electrode system was calibrated according to the method of Irving *et al.*,¹² and the pH-metric reading could therefore be converted into hydrogen ion concentration. The pK_w was found to be 13.76 under the conditions employed. The pH-metric titrations were performed throughout the pH range ≈ 2.0 –11.0, or below precipitation. All titrations started at pH *ca.* 2 by adding the necessary amount of acid. Samples of 25.00 or 10.00 cm^3 were used. The ligand concentrations were varied in the range 2.00×10^{-3} – $8.00 \times 10^{-3} \text{ mol dm}^{-3}$. Five or six different molybdate:ligand ratios were used ranging from 1:1 to 1:8.

An HP 8453 spectrophotometer was used to record the spectra in the region 200–500 nm. The concentration of MoO_4^{2-} was 5.00×10^{-4} – $1.00 \times 10^{-3} \text{ mol dm}^{-3}$; the metal:ligand ratio was 1:6 or 1:8.

The pH-metric data were used to find the stoichiometry of the species and calculate their stability constants. The calculations were performed by the PSEQUAD computer program¹³ using the log β data for polyoxomolybdates determined in our former work: $[HMoO_4]^-$, 4.03; H_2MoO_4 , 6.7; $[H_8(MoO_4)_7]^{6-}$, 53.18; $[H_9(MoO_4)_7]^{5-}$, 58.10; $[H_{10}(MoO_4)_7]^{4-}$, 62.11; $[H_{11}(MoO_4)_7]^{3-}$, 64.54.⁵

The 1H NMR measurements were performed on a Bruker AM360 instrument. The c_{ligand} was $1.00 \times 10^{-2} \text{ mol dm}^{-3}$, the metal to ligand ratio 1:3.

Preparation of $[MoO_2(Glyha)_2]$ and $[MoO_2(Sarha)_2]$

An aqueous solution (10 mL) of Glyha (0.18 g, 2 mmol) was added with stirring to an aqueous solution (10 mL) of sodium molybdate (0.242 g, 1 mmol) to give immediately a light yellow solution. The pH was then adjusted from 8.9 to 7.0 using 1 mol dm^{-3} HCl. Some excess of solvent was removed under reduced pressure and on cooling a lemon precipitate formed which was recrystallised by dissolving in the minimum volume of deionised water and layering with a 50:50 mixture of methanol–ethanol. Crystals were collected and washed with a little ethanol and diethyl ether and gave yellow $[MoO_2(O_2C_2N_2-$

$H_5)_2] \cdot 2.5H_2O$ suitable for single crystal X-ray diffraction studies. Data were collected using a Siemens SMART CCD area-detector diffractometer. The structure was solved by direct methods and refined by full-matrix least squares on F^2 for all data using SHELXL 97.¹⁴ Crystal data are given in Table 2.

CCDC reference number 186/1532.

See <http://www.rsc.org/suppdata/dt/1999/2789/> for crystallographic files in .cif format.

$[MoO_2(Sarha)_2]$ was prepared in the same way but the isolated compound was a powder in this case.

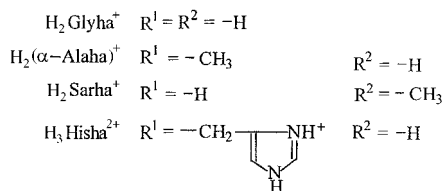
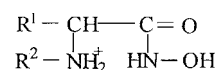
Computational details

Calculations were carried out using the GAUSSIAN94¹⁵ package on a Digital Au500 workstation, an Indigo origin 2000 system and a Dec alpha Viper system. Calculations were carried out using both Hartree–Fock and Density Functional (B3LYP) methods. All calculations reported were made using a 3-21G*¹⁶ basis set for both the metal and the ligand atoms. Attempts were made to extend these calculations using a Stuttgart ECP basis set for the molybdenum and the 6-311+G* basis for the rest of the atoms in the system; however calculations using this basis set required an unreasonable length of time to complete and were abandoned.

Results and discussion

Solution thermodynamic studies

The general formula of the totally protonated ligands is as shown.



The dissociation constants for the α -Alaha and Hisha ligands have been determined in our former studies,^{17,18} but all the macro constants have been measured again in the present work. The values, which agree well with formerly published ones,⁸ are shown in Table 1. Representative pH-metric titration curves of molybdenum(vi)-containing systems are shown on Fig. 1. Fig. 1(a) shows titration curves for the Mo^{VI} – β -Alaha model system for which the equilibrium results have been published.⁶ The curves clearly show that no measurable interaction occurs between Mo^{VI} and β -Alaha above pH *ca.* 6.5. The situation is

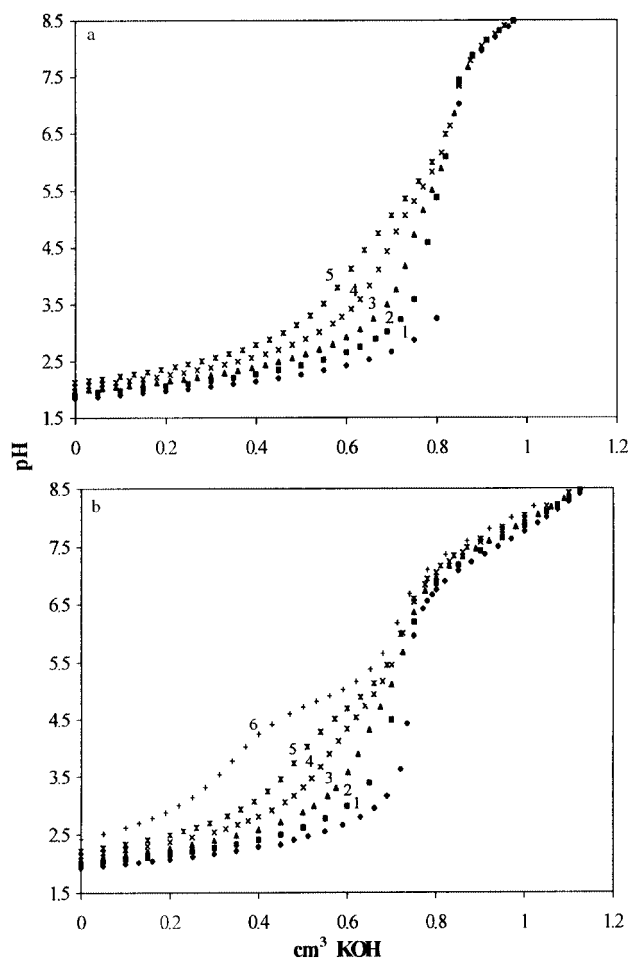


Fig. 1 pH-metric titration curves for: (a) β -Alaha and molybdenum(vi)- β -Alaha samples, $c_{\beta\text{-Alaha}} = 5.47 \times 10^{-3} \text{ mol dm}^{-3}$; (1) ligand only, (2) 1:5.5, (3) 1:2.8, (4) 1:1.8, (5) 1:1.5 molybdate to ligand ratio; (b) α -Alaha and molybdenum(vi)- α -Alaha samples, $c_{\alpha\text{-Alaha}} = 7.47 \times 10^{-3} \text{ mol dm}^{-3}$; (1) ligand only, (2) 1:7.6, (3) 1:3.8, (4) 1:2.5, (5) 1:1.9, (6) 1:1.3 molybdate to ligand ratio.

completely different in the case of α -Alaha (Fig. 1(b)), where the differences between the titration curves remain up to pH *ca.* 8.0–8.5 supporting interaction between the molybdenum(vi) and α -Alaha up to this pH. This pH value is about the same in the cases of Glyha and Hisha, but higher with Sarha. Precipitation hindered the studies on molybdenum(vi)-Hisha if the ligand to metal ratio was less than 4:1.

Calculations were performed from the pH-metric data. The models which yielded the best fittings and the calculated stability constants are summarised in Table 1. Based on the stability constants, the concentration distribution curves were calculated and those relating to Mo^{VI} - β -Alaha, - α -Alaha, -Sarha and -Hisha are shown in Figs. 2 and 3. The concentration distribution curves for the molybdenum(vi)- α -Alaha and -Glyha systems are very similar so only the former is presented here.

Comparing the pH-metric experimental findings and calculated results for molybdenum(vi)- α -Alaha and - β -Alaha systems, significant differences appear both in the equilibrium models (Table 1) and in the concentration distribution curves (Fig. 2). As found in our former work,⁶ the complexes $[\text{MoO}_2(\text{AH})_2]^{2+}$ and $[\text{MoO}_3(\text{AH})]$ formed in the molybdenum(vi)- β -Alaha system have the amino groups in their protonated form with normal O,O co-ordination of the hydroxamate function of β -Alaha. The stability constants calculated for the processes (1) and (2) were found to be comparable with the corresponding data of Aha.⁶

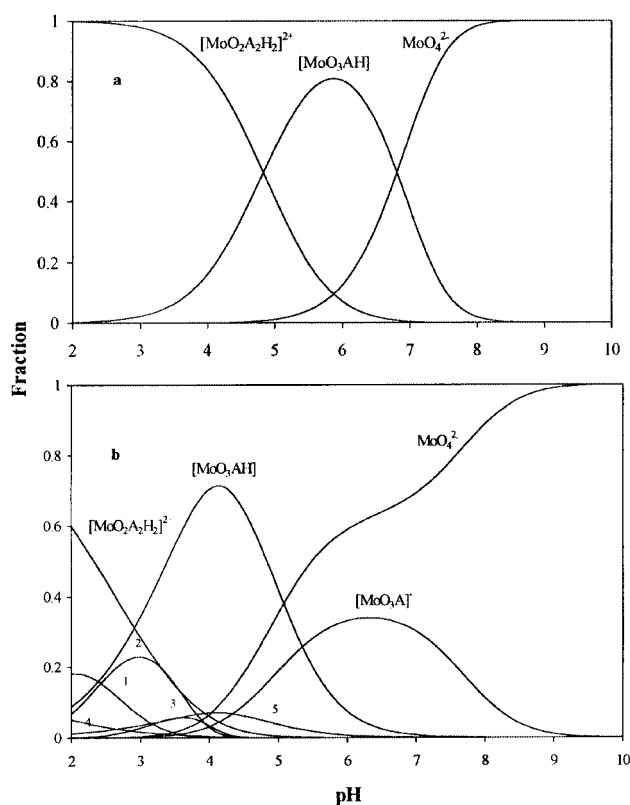
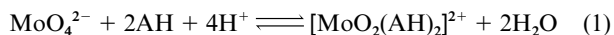


Fig. 2 Concentration distribution curves of complexes formed: (a) in the molybdenum- β -Alaha system, $c_{\beta\text{-Alaha}} = 6 \times 10^{-3} \text{ mol dm}^{-3}$; metal to ligand ratio 1:3; and (b) in the molybdenum- α -Alaha system, $c_{\alpha\text{-Alaha}} = 6 \times 10^{-3} \text{ mol dm}^{-3}$; metal to ligand ratio 1:3. (1) $[\text{H}_{11}(\text{MoO}_4)_7]^{3-}$; (2) $[\text{H}_{10}(\text{MoO}_4)_7]^{4-}$; (3) $[\text{H}_9(\text{MoO}_4)_7]^{5-}$; (4) H_2MoO_4 ; (5) $[\text{HMoO}_4]^-$.

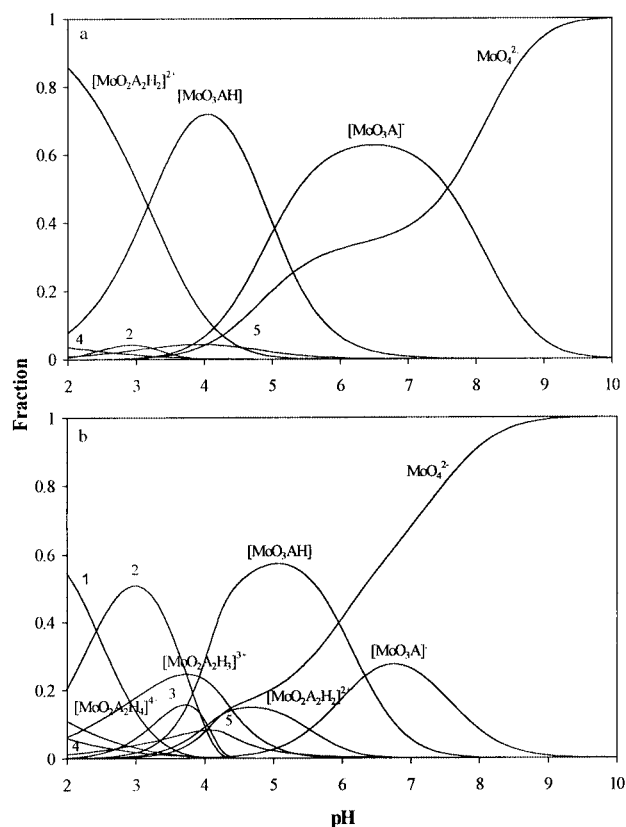


Fig. 3 Concentration distribution curves of complexes formed: (a) in the molybdenum-Sarha system, $c_{\text{Sarha}} = 6 \times 10^{-3} \text{ mol dm}^{-3}$; metal to ligand ratio 1:3; and (b) in the molybdenum-Hisha system, $c_{\text{Hisha}} = 6 \times 10^{-3} \text{ mol dm}^{-3}$; metal to ligand ratio 1:3. Species 1–5 as in Fig. 2.

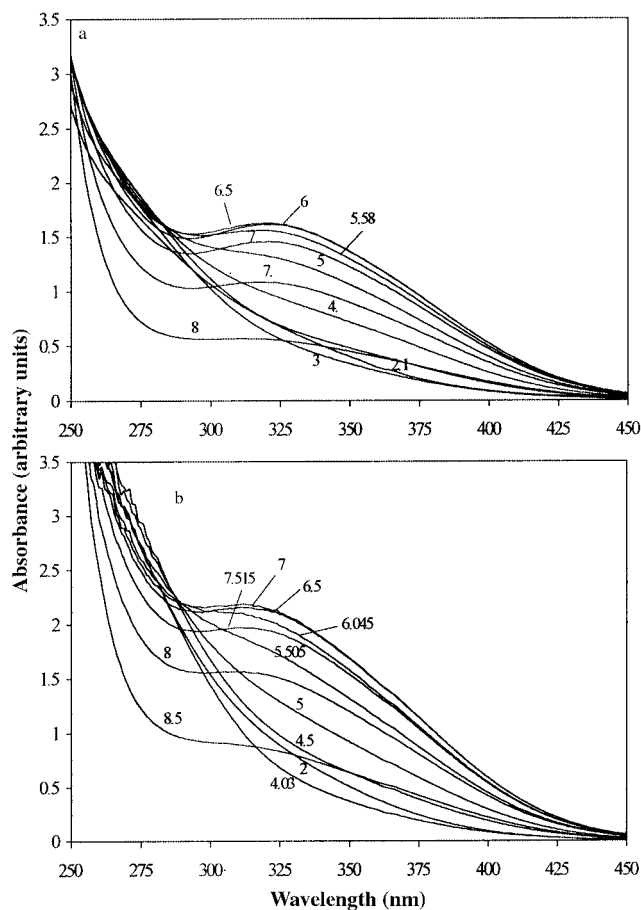
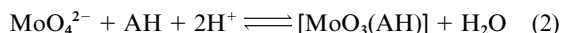


Fig. 4 The UV-visible spectra recorded at various pH values for (a) molybdenum(vi)- α -Alaha, $c_{\alpha\text{-Alaha}} = 8.00 \times 10^{-3} \text{ mol dm}^{-3}$, metal to ligand ratio 1:8, and for (b) molybdenum(vi)-Sarha, $c_{\text{Sarha}} = 6.00 \times 10^{-3} \text{ mol dm}^{-3}$, metal to ligand ratio 1:6.



Using the ligand dissociation constants,¹⁷ the (log) stability constants for reactions (1) and (2) were calculated for the Mo^{VI} - α -Alaha complexes. The values are 27.52 and 14.81. These are somewhat lower than those for β -Alaha, 30.58 and 16.22, and considerably lower than those for Aha, 32.46 and 17.16. It shows the lower stability of the α -Alaha complexes $[\text{MoO}_2(\text{AH})_2]^{2+}$ and $[\text{MoO}_3(\text{AH})]$ reflecting the lower basicity of the hydroxamate oxygens of α -Alaha which is caused, most probably, by the electron withdrawing effect of the NH_3^+ group in the α position. Evaluation of the stability constants for the above type of complexes formed by Glyha and Sarha gives similar conclusions. However, a new species, $[\text{MoO}_3\text{A}]^-$, is also formed in measurable concentration with α -Alaha, Glyha and Sarha, which contains the completely deprotonated α -derivative ligand and exists in the neutral and slightly basic pH range. This complex is not formed in the molybdenum(vi)- β -Alaha system since deprotonation of the NH_3^+ does not occur in the O,O co-ordinated β -Alaha.

It was found previously^{5,6} that a charge-transfer band characteristic of bis(hydroxamato)dioxomolybdenum(vi) occurs with λ_{max} at ca. 290 nm.⁶ Unfortunately, this band is almost covered by ligand bands in the cases of the α -amino acid derivatives. However, a new band appears with λ_{max} at ca. 320–325 nm, which does not occur if the ligand is β -Alaha, Aha or DFA.^{5,6} The spectra recorded for the molybdenum(vi)- α -Alaha and -Sarha systems at different pH values are shown in Fig. 4. (The results for molybdenum(vi)-Glyha are not shown as they are very similar to those for the molybdenum(vi)- α -Alaha.) Comparing the corresponding spectra and concentration distribution curves, the band with λ_{max} ca. 320 nm appears where

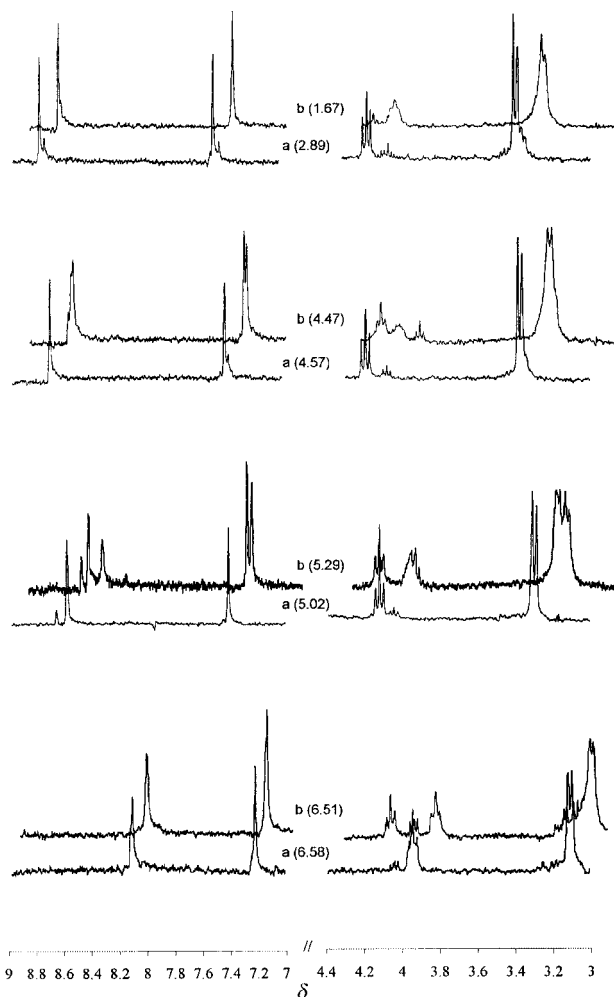


Fig. 5 The ^1H NMR spectra of (a) Hisha and (b) the Mo^{VI} -Hisha system at different pH values.

the $[\text{MoO}_3\text{A}]^-$ species starts to form in the molybdenum(vi)- α -Alaha, -Glyha and -Sarha systems and reaches its maximum absorbance value at the maximum concentration of $[\text{MoO}_3\text{A}]^-$ and decreases with decreasing concentration of $[\text{MoO}_3\text{A}]^-$.

From the above results one can conclude that, following O,O hydroxamate type co-ordination in the acidic pH range, co-ordination *via* the amino-N and hydroxamate-N donors of the α -aminohydroxamates occurs as the pH is raised. The stability of this 5-membered N,N-chelate is the highest with Sarha having the most basic amino N of the studied ligands,¹⁹ and results in the largest concentration of $[\text{MoO}_3\text{A}]^-$ in the molybdenum(vi)-Sarha system.

The situation is somewhat different if the ligand is Hisha. Not only the complexes $[\text{MoO}_2(\text{AH})_2]^{2+}$, $[\text{MoO}_3(\text{AH})]$ and $[\text{MoO}_3\text{A}]^-$ are formed, but also $[\text{MoO}_2(\text{AH}_2)_2]^{4+}$ and $[\text{MoO}_2(\text{AH})(\text{AH}_2)]^{3+}$, containing both or one of the imidazole N in the co-ordinated ligands in a protonated form. The ^1H NMR spectra for the ligand only (a) and the molybdenum(vi)-ligand (b) systems are presented in Fig. 5.

Taking all the results relating to the molybdenum(vi)-Hisha system together, the following conclusions can be drawn. The comparison of the ^1H NMR spectra for Hisha (a) and molybdenum(vi)-Hisha (b) at low pH, where $[\text{MoO}_2(\text{AH}_2)_2]^{4+}$, $[\text{MoO}_2(\text{AH})(\text{AH}_2)]^{3+}$ and $[\text{MoO}_2(\text{AH})_2]^{2+}$ complexes are formed, shows only the O,O co-ordination of the hydroxamate moiety (broadening of the methyl protons occurs) with the protons on the amino- and/or on the imidazole-N atoms. Between pH ca. 4 and 6, the co-ordination of the imidazole N is also probable as demonstrated by representative ^1H NMR spectra for pH ca. 4.5 and 5.3. In the pH range 4–6 the species

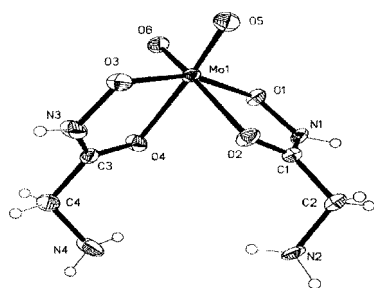


Fig. 6 Crystal structure of $[\text{MoO}_2(\text{Glyha})_2]$.

$[\text{MoO}_3(\text{AH})]$ dominates. It has its maximum concentration at pH *ca.* 5, where the absorbance of the UV band (λ_{max} 320 nm) is a maximum. The dissociable proton in $[\text{MoO}_3(\text{AH})]$ is situated either on the amino N or on the imidazole N. The microscopic dissociation constants of Hisha are not yet known, and their determination is in progress in our laboratory. However, the pH dependence of the ^1H chemical shifts of Hisha clearly supports the overlapped deprotonation of the amino and imidazole moieties. As a consequence, formation of two different co-ordination isomers of this species occurs. One of them has the ligand protonated on the amino N and co-ordinated in a tridentate manner *via* the two hydroxamate oxygens and the imidazole N. The other isomer contains the protonated imidazole N in the ligand which is co-ordinated most probably by the amino- and hydroxamate-N donors. The band with an absorption maximum at *ca.* 320 nm remains in the UV-vis spectra during the pH range where $[\text{MoO}_3\text{A}]^-$ is formed. This finding is consistent with the corresponding results for Glyha, α -Alaha and Sarha containing systems supporting the co-ordination of Hisha *via* the 5-membered N,N-chelate.

Crystal structure of $[\text{MoO}_2(\text{Glyha})_2]$

In view of the above equilibrium studies and resultant species distribution curves which show the presence of both O,O and N,N co-ordination species over the pH range 2–8, attempts were made to isolate pure solid compounds at the appropriate pH values. Unfortunately, despite repeated attempts using a range of solvents and pH values the only pure compounds to be isolated were $[\text{MoO}_2(\text{Sarha})_2]$ as a powder and $[\text{MoO}_2(\text{Glyha})_2]$ as crystals formed by the reaction of glycine hydroxamic acid (Glyha) and sodium molybdate dihydrate ($\text{Na}_2\text{MoO}_4 \cdot 2\text{H}_2\text{O}$) in a 2:1 ratio in aqueous solution at a pH of 7.0. The yellow crystals were grown by dissolving the bright yellow powder in the minimum of deionised water and layering with a 50:50 mixture of methanol-ethanol and again with diethyl ether; after a couple of hours yellow crystals formed suitable for X-ray analysis.

The crystal structure of $[\text{MoO}_2(\text{Glyha})_2]$ is shown in Fig. 6 with crystallographic data and selected parameters in Tables 2, 3 and 4. The structure shows clearly that O,O hydroxamate bonding occurs in contrast to N,N bonding involving deprotonation of the hydroxamate nitrogen and the α -amino nitrogen previously observed in complexes of nickel(II), copper(II) and cobalt(II).^{7,8} The bond distances and angles in the co-ordination sphere of molybdenum in $[\text{MoO}_2(\text{Glyha})_2]$ are very close to those previously reported for $[\text{MoO}_2\{\text{CH}_3(\text{CH}_2)_n\text{CONHO}\}_2]$ ($n = 4$ or 5).⁴ For example, the Mo–O (ligand) bonds *trans* to the terminal Mo–O bonds are again elongated compared to the *cis* Mo–O (ligand) bonds, *e.g.* Mo–O(1) 2.001(4) Å, whereas Mo–O(2) 2.140(4), Mo–O(3) 1.982(4) and Mo–O(4) 2.145(4) Å. These distances are very close to the analogous Mo–O(2) 2.019(8) and Mo–O(1) 2.191(7) Å in $[\text{MoO}_2\{\text{CH}_3(\text{CH}_2)_4\text{CONHO}\}_2]$.⁴ Bond angles are also very similar in the series. A *cis* arrangement of the MoO_2 grouping also occurs in both $[\text{MoO}_2(\text{Glyha})_2]$ and $[\text{MoO}_2\{\text{CH}_3(\text{CH}_2)_n\text{CONHO}\}_2]$ ($n = 4$ or 5).

Table 2 Crystal data and structure refinement for complex $[\text{MoO}_2(\text{Glyha})_2] \cdot 2.5\text{H}_2\text{O}$

Empirical formula	$\text{C}_4\text{H}_{15}\text{MoN}_4\text{O}_{8.5}$
Formula weight	351.14
<i>T</i> /K	180(2)
Crystal system	Monoclinic
Space group	$P2_1/n$
<i>a</i> /Å	7.0100(2)
<i>b</i> /Å	13.7821(3)
<i>c</i> /Å	12.6683(2)
β /°	105.3000(10)
<i>V</i> /Å ³ , <i>Z</i>	1180.54(5), 4
Reflections collected	6009
Independent reflections	2064 ($R_{\text{int}} = 0.0439$)
Final <i>R</i> 1, <i>wR</i> 2 [<i>I</i> > 2 σ (<i>I</i>)]	0.0492, 0.1248 (for 1716 reflections) 0.0606, 0.1292
Largest difference peak and hole/e Å ^{−3}	1.484 and −1.421

Table 3 Bond lengths (Å) and angles (°) of $[\text{MoO}_2(\text{Glyha})_2] \cdot 2.5\text{H}_2\text{O}$

Mo(1)–O(5)	1.706(5)	Mo(1)–O(6)	1.723(5)
Mo(1)–O(3)	1.982(4)	Mo(1)–O(1)	2.001(4)
Mo(1)–O(2)	2.140(4)	Mo(1)–O(4)	2.145(4)
N(1)–C(1)	1.275(8)	N(1)–O(1)	1.424(7)
N(2)–C(2)	1.495(9)	N(3)–C(3)	1.293(8)
N(3)–O(3)	1.426(7)	N(4)–C(4)	1.475(9)
O(2)–C(1)	1.307(8)	O(4)–C(3)	1.285(7)
C(1)–C(2)	1.508(9)	C(3)–C(4)	1.504(9)
O(5)–Mo(1)–O(6)	102.9(2)	O(5)–Mo(1)–O(3)	88.2(2)
O(6)–Mo(1)–O(3)	107.7(2)	O(5)–Mo(1)–O(1)	105.1(2)
O(6)–Mo(1)–O(1)	86.6(2)	O(3)–Mo(1)–O(1)	158.0(2)
O(5)–Mo(1)–O(2)	93.2(2)	O(6)–Mo(1)–O(2)	157.2(2)
O(3)–Mo(1)–O(2)	88.6(2)	O(1)–Mo(1)–O(2)	73.6(2)
O(5)–Mo(1)–O(4)	161.3(2)	O(6)–Mo(1)–O(4)	88.8(2)
O(3)–Mo(1)–O(4)	74.2(2)	O(1)–Mo(1)–O(4)	89.9(2)
O(2)–Mo(1)–O(4)	80.2(2)	C(1)–N(1)–O(1)	109.5(5)
C(3)–N(3)–O(3)	110.1(5)	N(1)–O(1)–Mo(1)	120.4(3)
C(1)–O(2)–Mo(1)	113.0(4)	N(3)–O(3)–Mo(1)	119.8(3)
C(3)–O(4)–Mo(1)	113.1(4)	N(1)–C(1)–O(2)	123.3(6)
N(1)–C(1)–C(2)	118.0(6)	O(2)–C(1)–C(2)	118.7(6)
N(2)–C(2)–C(1)	109.4(5)	O(4)–C(3)–N(3)	122.7(6)
O(4)–C(3)–C(4)	119.6(6)	N(3)–C(3)–C(4)	117.7(5)
N(4)–C(4)–C(3)	109.1(6)		

Theoretical studies

In view of the above structural proof of O,O co-ordination of glycine hydroxamic acid with Mo^{VI} and the existence of a number of solution species which are considered to contain variously O,O and N,N bonding, it was decided to compute the respective energies of the various co-ordination isomers for both the structurally characterised $[\text{MoO}_2(\text{Glyha})_2]$ species and the $[\text{MoO}_3\text{A}]^-$ solution species which is formed around neutral pH for α -Alaha, Glyha and Sarha. Calculations were carried out for both species for Glyha and Sarha and the results are given in Table 5. In the case of $[\text{MoO}_2(\text{Glyha})_2]$ and $[\text{MoO}_2(\text{Sarha})_2]$ the energies of the two co-ordination isomers were calculated using both the HF/3-21G* and B3LYP/3-21G* *ab initio* methods and the relative order of the energies was found to be the same using both of the above computational methods, *i.e.* $E(\text{O},\text{O}) < E(\text{N},\text{N})$. The fact that this order was reproducible by the simpler and quicker computational method (HF/3-21G*) gave us confidence to apply only this method to the complete range of species studied. However, even with this simplification it was not possible to perform computations for the analogous complexes of histidine hydroxamic acid without excessive computer time being required.

The calculated energies of the O,O and N,N isomers of $[\text{MoO}_2(\text{Glyha})_2]$ and $[\text{MoO}_2(\text{Sarha})_2]$ are given in Table 5. Their relative closeness is in accord with the above solution studies which show the presence of O,O and N,N isomers with varying pH. At the same time the calculated energies show that the O,O

Table 4 Hydrogen bonds with $H \cdots A \angle r(A) + 2.000 \text{ \AA}$ and $\langle \text{DHA} \rangle 110^\circ$

D-H	$d(\text{D-H})$	$d(\text{H} \cdots \text{A})$	$\angle \text{DHA}$	$d(\text{D} \cdots \text{A})$	A
N1-H1A	0.880	2.107	151.87	2.913	$\text{N4}[-x + 1, -y + 1, -z + 1]$
N1-H1A	0.880	2.594	134.11	3.268	$\text{O4}[-x + 1, -y + 1, -z + 1]$
N2-H2C	0.754	2.080	174.76	2.832	$\text{O1}[-x + 1, -y + 1, -z + 1]$
N2-H2D	0.757	2.075	166.14	2.816	$\text{O1S}[x + \frac{1}{2}, -y + \frac{3}{2}, -z + \frac{1}{2}]$
N3-H3A	0.880	2.031	151.02	2.833	$\text{N2}[-x + \frac{3}{2}, y + \frac{1}{2}, -z + \frac{3}{2}]$
N4-H4C	0.782	2.261	115.36	2.690	O4S
N4-H4C	0.782	2.372	136.22	2.986	$\text{O1S}[x + \frac{1}{2}, -y + \frac{3}{2}, z + \frac{1}{2}]$
N4-H4C	0.782	2.562	135.12	3.164	$\text{O5}[x - \frac{1}{2}, -y + \frac{3}{2}, z + \frac{1}{2}]$
N4-H4D	0.783	2.216	148.55	2.913	$\text{N1}[-x + 1, -y + 1, -z + 1]$

Table 5 Theoretical relative energies in kJ mol^{-1}

$[\text{MoO}_2(\text{Glyha})_2]$	Octahedral	
Co-ordination	$[\text{O}, \text{O}]$	$[\text{N}, \text{N}]$
HF/3-21G*	0.00	62.38
B3LYP/3-21G*	0.00	57.32
$[\text{MoO}_2(\text{Sarha})_2]$		
Co-ordination	$[\text{O}, \text{O}]$	$[\text{N}, \text{N}]$
HF/3-21G*	0.00	75.02
B3LYP/3-21G*	0.00	57.99
$[\text{MoO}_3(\text{Glyha})]^-$	Trigonal bipyramidal	
Co-ordination	$[\text{O}, \text{O}]$	$[\text{N}, \text{N}]$
HF/3-21G*	31.80	0.00
$[\text{MoO}_3(\text{Sarha})]^-$	Trigonal bipyramidal	
Co-ordination	$[\text{O}, \text{O}]$	$[\text{N}, \text{N}]$
HF/3-21G*	31.63	0.00

isomer is the more stable in accord with the crystal structure of $[\text{MoO}_2(\text{Glyha})_2]$ (Fig. 6); however, because of the closeness of the calculated energies of the isomers for an isolated species in the gas phase the formation of a particular isomer in the solid state may well be influenced by the extent of intermolecular hydrogen bonding, the presence of which in $[\text{MoO}_2(\text{Glyha})_2] \cdot 2\text{H}_2\text{O}$ is clearly extensive as shown in Table 4 and has also been reported in the N,N bonded $[\text{Ni}(\text{Glyha})_2]$.⁷

In the case of the $[\text{MoO}_3\text{A}]^-$ species the above calculated order of stabilities is reversed *i.e.* the N,N co-ordination isomer is slightly more stable than the O,O isomer for both Glyha and Sarha. Unfortunately, we were not able to isolate stable solid samples of either of the $[\text{MoO}_3\text{A}]^-$ species even using large cations such as $[\text{NBu}_4]^+$ in an attempt to stabilise the anions; however, the order of calculated energies is in good agreement with the above equilibrium studies which show clear evidence for the presence of the $[\text{MoO}_3\text{A}]^-$ species as the pH is raised with that formed by Sarha being the more stable (Table 1).

Conclusion

In the metal complexes of the hydroxamic acid derivatives of α -amino acids formation of co-ordination isomers is possible; O,O co-ordination can occur through the hydroxamate oxygens, while the N,N form occurs *via* the amino- and hydroxamate-N donors. The stabilities of these different types of chelates strongly depend on the character of the metal ion. O,O Co-ordination exclusively occurs with typically hard metal ions (*e.g.* iron(III), aluminium(III), gallium(III)), but N,N isomers dominate in other cases (*e.g.* nickel(II), cobalt(II)). An interesting change occurs in the co-ordination mode with changing pH in the cases of copper(II) (former work) and molybdenum(VI). One proton per ligand is replaced by the molybdenum in the acidic pH range and O,O isomers are formed. Two protons must be replaced if the N,N chelate is formed resulting in a much more significant pH dependence of the conditional

stability of this latter chelate. Its formation, however, was found at and somewhat above neutral pH. The relative closeness of the calculated energies of the O,O and N,N bonded isomers supports the solution equilibrium results. Up to now only $[\text{MoO}_2(\text{Glyha})_2]$ has been isolated and found suitable for a crystal structure determination which confirmed the O,O co-ordination of the ligand.

Acknowledgements

We thank EU COST D8 and OTKA T023612 (E. F.) for support.

References

- 1 A. K. Duhme, Z. Dauter, R. C. Hider and S. Pohl, *Inorg. Chem.*, 1996, **35**, 3059.
- 2 M. Albrecht, S. J. Franklin and K. N. Raymond, *Inorg. Chem.*, 1994, **33**, 5785.
- 3 P. Ghosh and A. Chakravorty, *Inorg. Chem.*, 1983, **22**, 1322.
- 4 D. A. Brown, H. Bogge, R. Coogan, D. Doocey, T. J. Kemp, A. Müller and B. Neumann, *Inorg. Chem.*, 1996, **35**, 1674.
- 5 E. Farkas, H. Csóka, G. Micera and A. Dessi, *J. Inorg. Biochem.*, 1997, **65**, 281.
- 6 E. Farkas, K. Megyeri, L. Somsák and L. Kovács, *J. Inorg. Biochem.*, 1998, **70**, 41.
- 7 D. A. Brown, A. L. Roche, T. A. Pakkanen, T. T. Pakkanen and K. Smolander, *J. Chem. Soc., Chem. Commun.*, 1982, 676.
- 8 B. Kurzak, H. Kozłowski and E. Farkas, *Coord. Chem. Rev.*, 1992, **114**, 169.
- 9 E. Farkas, E. Kozma, T. Kiss, I. Tóth and B. Kurzak, *J. Chem. Soc., Dalton Trans.*, 1995, 477.
- 10 E. Farkas and I. Sóvágó, in *Amino Acids, Peptides and Proteins*, Specialist Periodical Report, J. S. Davies (senior reporter), The Royal Society of Chemistry, Cambridge, 1998, vol. 29.
- 11 A. H. Blatt, *Organic Syntheses*, Wiley, New York, 1963.
- 12 H. Irving, M. G. Miles and L. D. Pettit, *Anal. Chim. Acta*, 1967, **38**, 475.
- 13 L. Zékány and I. Nagypál, in *Computational Methods for the Determination of Stability Constants*, ed. D. Legett, Plenum, New York, 1985.
- 14 G. M. Sheldrick, SHELXL 97, Program for the Refinement of Crystal Structures, University of Göttingen, 1997.
- 15 Gaussian 94, Revision C.3, M. J. Frisch, G. W. Trucks, H. B. Schlegel, P. M. W. Gill, B. G. Johnson, M. A. Robb, J. R. Cheeseman, T. Keith, G. A. Peterson, J. A. Montgomery, K. Raghavachari, M. A. Al-Laham, V. G. Zakrzewski, J. V. Ortiz, J. B. Foresman, J. Cioslowski, B. B. Stefanov, A. Nanayakkara, M. Challacombe, C. Y. Peng, P. Y. Ayala, W. Chen, M. W. Wong, J. L. Andres, E. S. Replogle, R. Gomperts, R. L. Martin, D. J. Fox, J. S. Binkley, D. J. Defrees, J. Baker, J. P. Stewart, M. Head-Gordon, C. Gonzalez and J. A. Pople, Gaussian, Inc., Pittsburgh, PA, 1995.
- 16 K. D. Dobbs and W. J. Hehre, *J. Comput. Chem.*, 1987, **8**, 861.
- 17 E. Farkas, T. Kiss and B. Kurzak, *J. Chem. Soc., Perkin Trans. 2*, 1990, 1255.
- 18 E. Farkas and B. Kurzak, *J. Coord. Chem.*, 1990, **22**, 145.
- 19 B. Kurzak, H. Kozłowski and P. Decock, *J. Inorg. Biochem.*, 1991, **41**, 71.